

Supporting Information

A Novel Synthetic Strategy for Magnetite-Type Compounds.

A Combined Experimental and DFT-Computational Study.

Luigi Cigarini¹, Davide Vanossi¹, Federica Bondioli^{2,3}, Claudio Fontanesi^{1*}.

¹University of Modena and Reggio Emilia, DSCG, Via G. Campi 41125, Modena, ITALY

²University of Parma, Department of Industrial Engineering, Viale Parco Area delle Scienze, 181/A,
43124 Parma (Italy)

³Consorzio INSTM, Via G. Giusti 9, 51121 Firenze (Italy)

1. Calculated IR Spectra

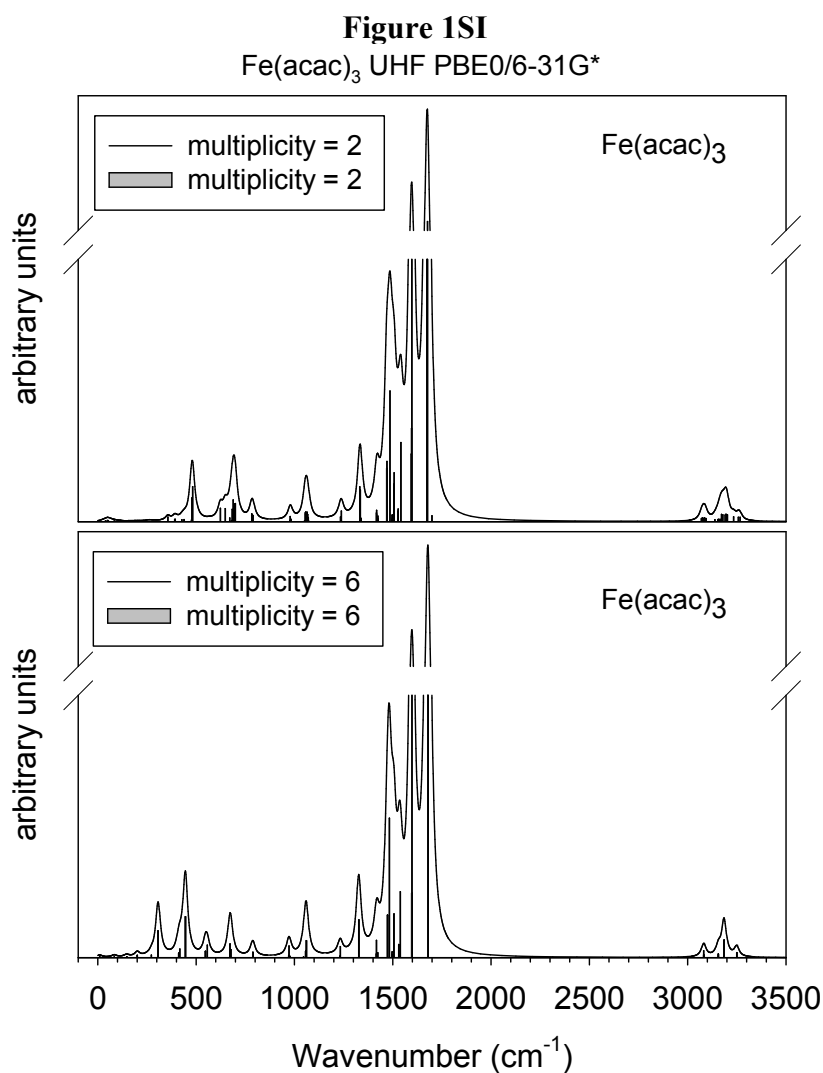


Figure 1 SI. IR absorption spectra, UPBE0/6-31G* level of the theory, have been calculated for both the multiplicity 2 and 6; full optimization without symmetry constraint. Calculations run with D3 symmetry produced the same results.

Note that, our calculated IR spectra are also in tight agreement with the data, theoretical and experimental, published by Pulay.¹

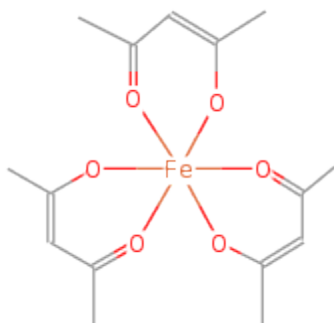


Figure 2 SI

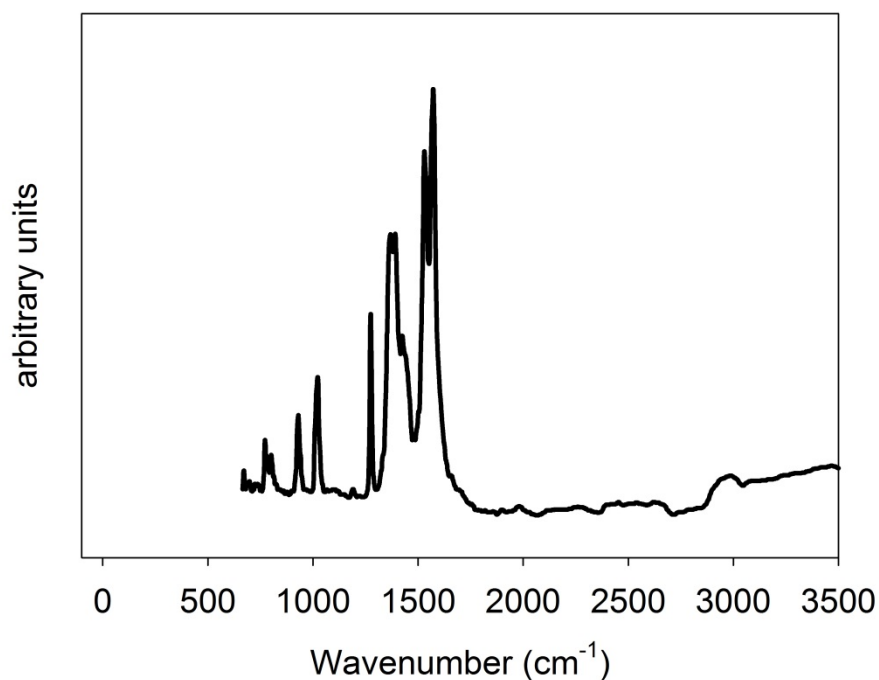
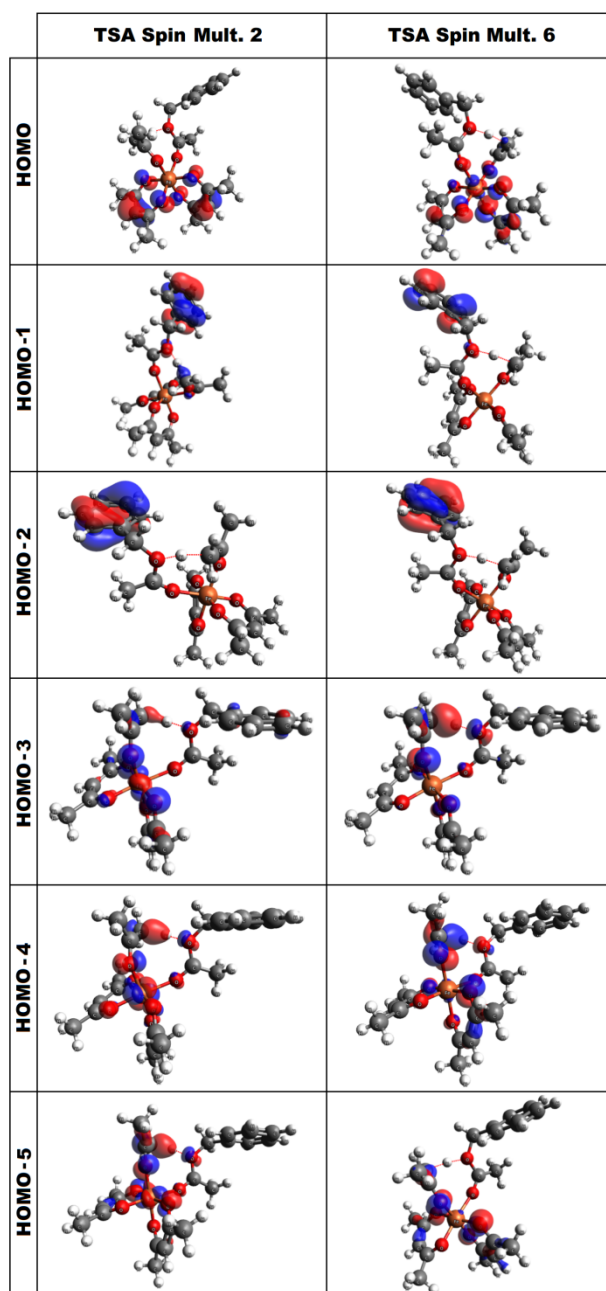


Figure 2 SI. Experimental absorption IR spectrum. Freely available from the NIST website: <http://webbook.nist.gov/cgi/cbook.cgi?ID=C14024181&Mask=80#IR-Spec>

2. SPIN multiplicity

Figure 3 SI. Comparison of the first six occupied MOs, TSA as a function of spin multiplicity. Spin multiplicity = 2 left panel. Spin multiplicity = 6 right panel. Qualitatively the same moieties are involved in a quite similar ways in the MOs. Maintaining also the same ordering in energy.



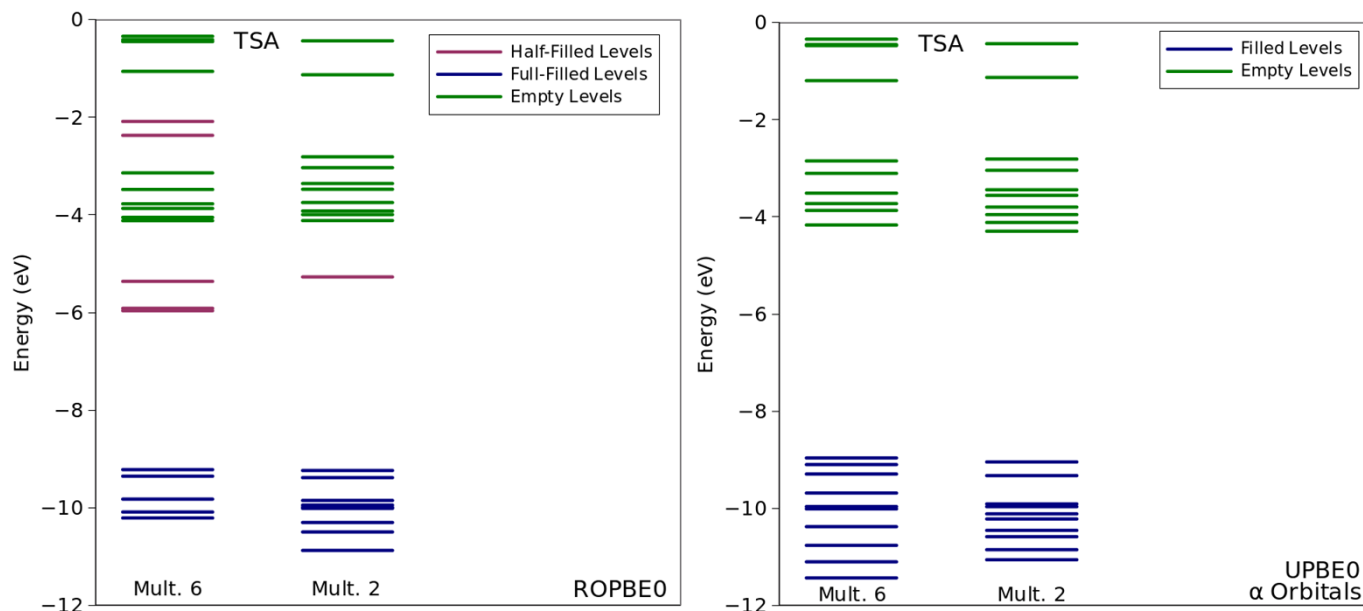


Figure 4 SI. Comparison of the frontier MO energies, TSA, as a function of spin multiplicity. Left panel Restricted open-shell. Right panel Unrestricted open-shell.

3. Check on DFT energy reliability.

The comparison of DFT and CASPT2 theoretical results suggests that density functional calculations are able to yield reliable energies, as well optimized structures, in the case of chemical processes involving iron (and transition metals as well).²⁻⁵ To further clarify this point, the energy pattern of the reaction pathway shown in Figure 3, acid environment (compare the main manuscript), has been checked performing UMP4SDQ(FC)/6-31g* single points calculations (i.e. using the same geometry corresponding to Figure 3 main manuscript), Figure 5 SI.

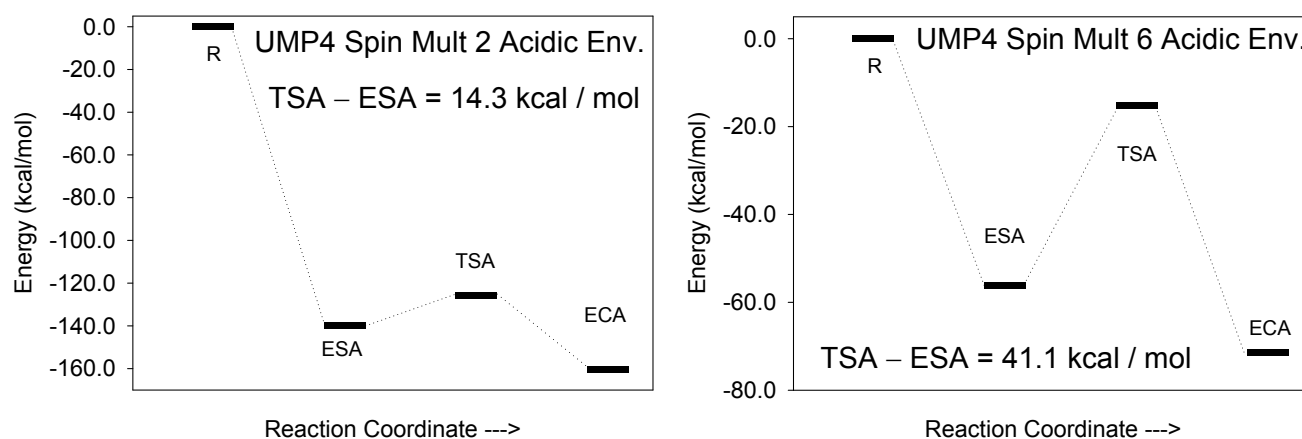


Figure 5 SI. Reaction path energy pattern calculated at the UMP4SDQ(FC)/6-31G* level of theory. Left panel: multiplicity = 2. Right panel: multiplicity = 6. Compare the main manuscript for details.

Table 1SI	Activation Energy $E_{TSA} - E_{ESA}$ kcal / mol	
	PBE0/6-31G*	UMP4SDQ(FC)/6-31G*
Acid env. Mult = 2	7.5	14.3
Acid env. Mult = 6	39.5	41.1

Moreover, UMP4SDQ(FC)/6-31g* calculations were also performed to check the difference in energy between structures indicated as point 1 and point 2 of Figure 7 (DRC) in the main manuscript. Single point UMP4(FC)/6-31G* results yield:

Multiplicity 2, -2640.8107727 hartree (point1), -2641.0321374 hartree (point 2) $\Delta E = 138.9$ kcal / mol

Multiplicity 6, -2640.8990640 hartree (point1), -2641.0943601 hartree (point 2) $\Delta E = 122.6$ kcal /

PBE0/6-31G* yield differences in energy values (see Figure 4 DRC in the main manuscript, ΔE is about 135 kcal / mol) which compare well to UMP4 ones.

4. Solvent effect SMD

The SMD⁶ solvation model (single point, i.e. using the same geometry corresponding to Figure 3 main manuscript), as implement in the Gaussian program, has been used to calculate the energy pattern concerning the reaction pathway shown in Figure 3, acid environment (compare the main manuscript), Figure 6 SI.

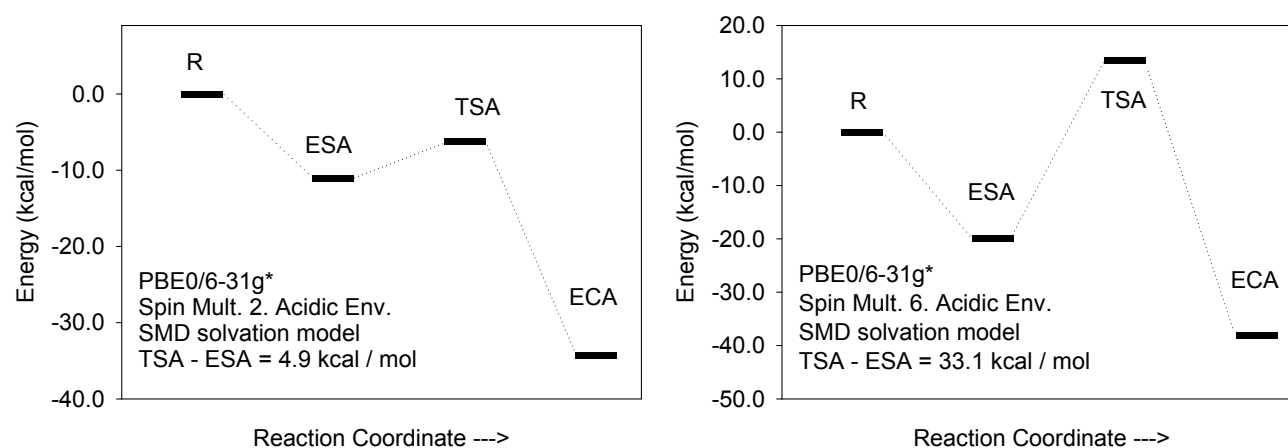


Figure 6 SI. Reaction path energy pattern calculated at the PBE0/6-31G* level of theory, with inclusion of SMD solvent. Left panel: multiplicity = 2. Right panel: multiplicity = 6. Compare the main manuscript for details.

5. Further analysis on system's potential energy hyper-surface

The hypothesis of existence of alternative reaction paths in addition to the studied ones has been carefully taken into account. In particular, not pretending our analysis to be exhaustive, a very interesting result has been found for the system in simulated acidic medium: the coordination of a protonated solvent molecule, by means of its two hydroxylic protons, to carbonylic oxygens situated on different acetylacetonate ligands of the same reagent complex, appears to be a very energetically favourable condition. The resulting configuration, which is shown in Figure 7 SI and it is referred as X intermediate, could probably produce, when attacked by a second molecule of solvent, maybe protonated or not, a different transition state for the first stage of the reaction, which would be alternative to TSA. In our opinion this hypothesis should be furtherly investigated in future, first of all with the determination of this hypothetical alternative transition state. This would provide another justification to the point, already clear from the results of our calculations, that the presence of acidic medium is the determinant factor for the increase in reaction rate observed.

Figure 7 SI X Intermediate

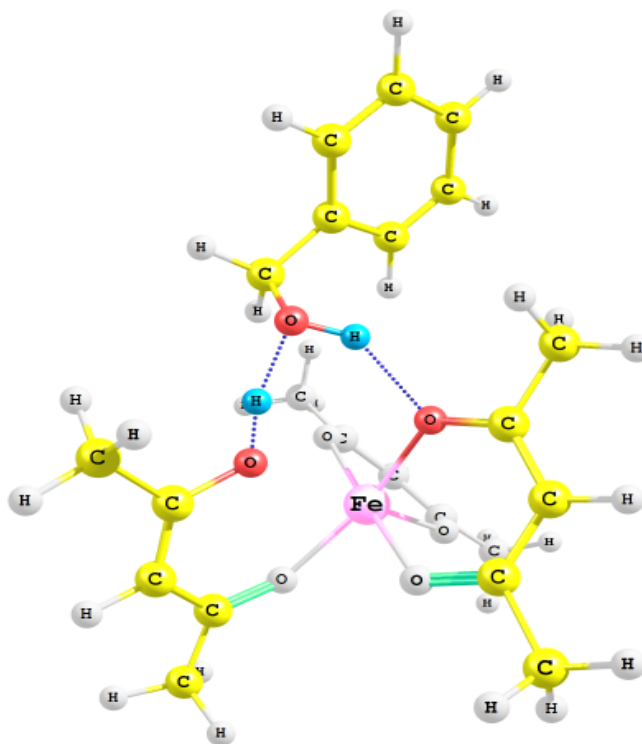


Figure 8 SI

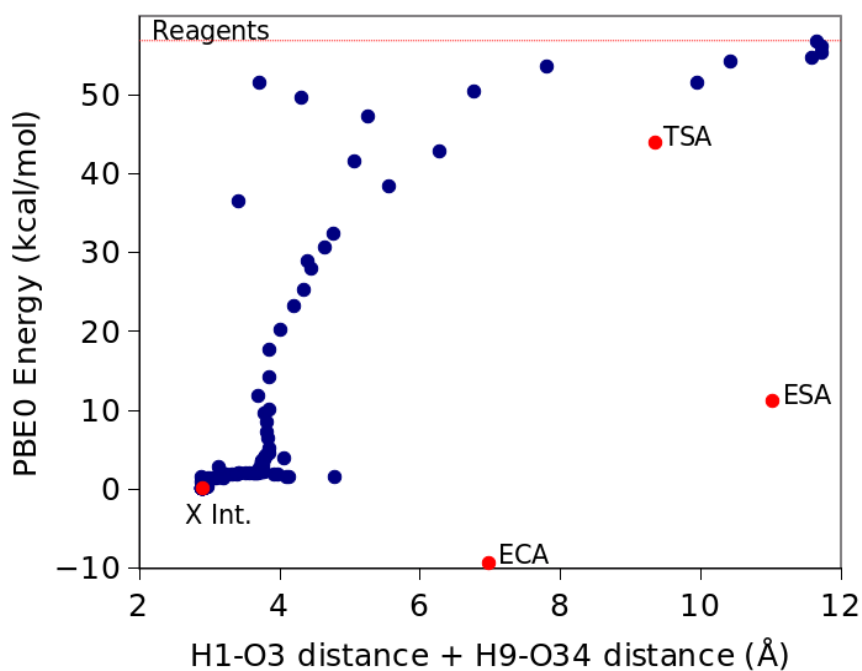


Figure 8 SI. The graph shows a projection of some points of the potential energy hypersurface, for the simulated acidic medium system, over a relevant combination of coordinates (see legend in Figure 5 in the main manuscript). X intermediate energy is used as the zero on the energy scale. Blue dots are non stationary intermediate structures spanned during various geometrical optimization runs, from which X Intermediate was obtained as a result. Red dots are stationary points: the X Intermediate stationary point, and other intermediates already discussed in this work and reported here for a comparison, also the reagents level energy is reported as a red dotted line. All the results reported in this graphic are calculated setting up spin multiplicity 6, PBE0/6-31G*.

6. DRC in neutral medium

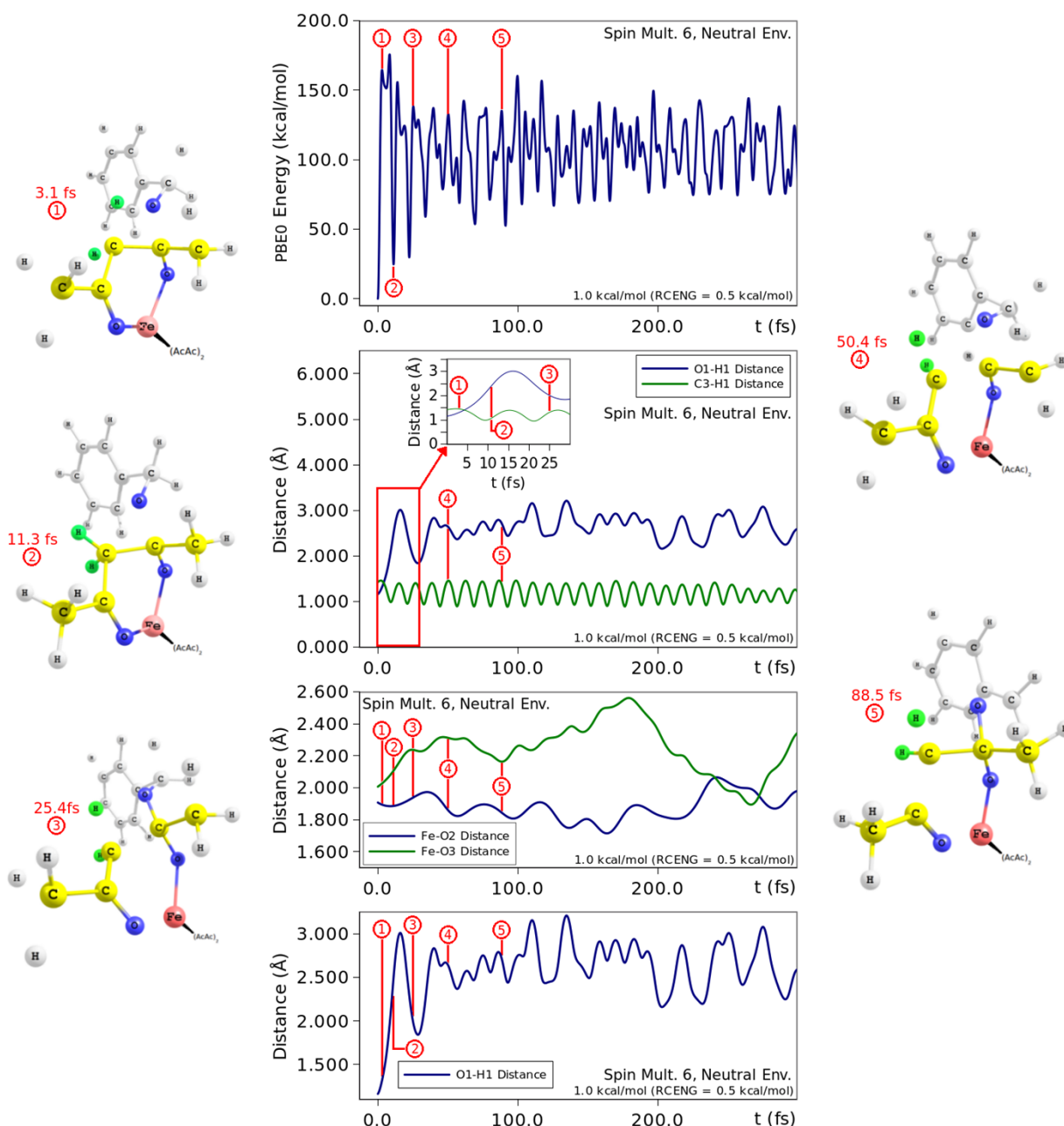


Figure 9 SI. (a) PBE0 electronic energy (potential energy) as a function of simulated time for a DRC calculation starting from TSN and performed with an imposed electron spin multiplicity of 6 and with a total nuclear kinetic energy distributed to the system at the start of 1.0 kcal/mol, half of which attributed to the intrinsic reaction coordinate normal mode (RCENG). (b) Evolution of two geometrical parameters of the system (O-H and C-H bond lengths involved in the reaction) over simulated time of the same DRC calculation above-mentioned. (c) Fe-O bond lengths involved in the reaction plotted as a function of the simulated time from the same DRC calculation showed in the above graphs. (d) Plot of the O-H bond length involved in the reaction over the simulated time from the same DRC calculation described above. (Left and right) Five visualizations of the system (spatial positions of the nuclei) at different simulated times in the DRC calculation previously described and presented in the central graphs.

References

- 1 I. Diaz-Acosta, J. Baker, W. Cordes and P. Pulay, *J. Phys. Chem. A*, 2001, **105**, 238–244.
- 2 P. Wählén, C. Danilo, V. Vallet, F. Réal, J.-P. Flament and U. Wahlgren, *J. Chem. Theory Comput.*, 2008, **4**, 569–577.
- 3 F. Bernardi, A. Bottoni, R. Casadio, P. Fariselli and A. Rigo, *Int. J. Quantum Chem.*, 1996, **58**, 109–119.
- 4 Z. Liu, L. Zhong, Y. Yang, R. Cheng and B. Liu, *J. Phys. Chem. A*, 2011, **115**, 8131–8141.
- 5 T. Takatani, J. S. Sears and C. D. Sherrill, *J. Phys. Chem. A*, 2009, **113**, 9231–9236.
- 6 A. V. Marenich, C. J. Cramer and D. G. Truhlar, *J. Phys. Chem. B*, 2009, **113**, 6378–6396.